ULUSLARARASI 3B YAZICI TEKNOLOJİLERİ
VE DİJİTAL ENDÜSTRİ DERGİSİ

INTERNATIONAL JOURNAL OF 3D PRINTING
TECHNOLOGIES AND DIGITAL INDUSTRY

ISSN:2602-3350 (Online)

URL: https://dergipark.org.tr/ij3dptdi

CHARACTERIZATION OF 3D PRINTED CONDUCTIVE FLEXIBLE MATERIALS FOR SOFT ROBOTIC APPLICATIONS

Yazarlar (Authors): Ozan Arslan, Ozgun Selvi*, Onat Halis Totuk

Bu makaleye şu şekilde atıfta bulunabilirsiniz (To cite to this article): *Arslan O., Selvi O., Totuk O. H., "Characterization of 3D Printed Conductive Flexible Materials for Soft Robotic Applications" Int. J. of 3D Printing Tech. Dig. Ind., 8(1): 1-7, (2024).*

DOI: 10.46519/ij3dptdi.1349314

Araştırma Makale/ Research Article

Erişim Linki: (To link to this article): https://dergipark.org.tr/en/pub/ij3dptdi/archive

CHARACTERIZATION OF 3D PRINTED CONDUCTIVE FLEXIBLE MATERIALS FOR SOFT ROBOTIC APPLICATIONS

Ozan Arslan[a], Ozgun Selvi[b*], Onat Halis Totuk[c]

[a] Turkish Aerospace Industries, ANKARA
[b]University of Central Lancashire, School of Engineering and Computing, Preston, United Kingdom
[c]Çankaya University, Engineering Faculty, Mechanical Engineering Department, ANKARA

[*] *Corresponding Author: oselvi@uclan.ac.uk*

(**Received:** 24.08.23; **Revised:** 21.11.23; **Accepted:** 04.01.24)

ABSTRACT

Soft robots composed of compliant and flexible materials can safely interact with humans and adapt to unstructured environments. However, integrating sensors, actuators, and control circuits into soft structures remains challenging. Additive manufacturing shows promise for fabricating soft robots with embedded electronics using conductive flexible composites. Nevertheless, there is still a limited understanding of the electromechanical behavior of 3D-printed conductive structures when subjected to the types of strains relevant to soft robotics applications. Optimized design requires characterizing the interplay between a soft component's changing shape and electrical properties during deformation. This study investigates the application of 3D printing technology to fabricate various geometries using a conductive, flexible material for soft robotic applications. The primary objective is to understand and characterize the behavior of differently shaped 3D-printed conductive materials under various mechanical stresses. Two distinct test setups are designed for conducting bending and tensile tests on the produced materials. Diverse geometries are printed using the conductive flexible material with desirable mechanical and electrical properties to employ tensile and bending tests. The experiments reveal a direct correlation between shape change and electrical resistance of the 3D printed materials, providing valuable insights into their adaptability for soft robotics. According to numerical results, honeycomb profiles are found to be the most linear and stable profile type. This research not only contributes to the field of flexible conductive materials but also lays the foundation for integrating these materials into future engineering designs, potentially enabling the development of highly responsive and adaptable devices for various industries.

Keywords: Soft Robotics, Characterization, Conductive Filament, 3D Printed.

1. INTRODUCTION

Soft robotics is a rapidly growing field that aims to create robots that can interact with complex and dynamic environments, such as the human body, natural habitats, and industrial settings[1]. Soft robots are typically made of flexible and deformable materials that can change their shape and functionality in response to external stimuli, such as mechanical stress, temperature, or electric fields [2-4]. One of the advantages of soft robots is that they can achieve high levels of adaptability, compliance, and safety, which are desirable for applications such as biomedical devices, wearable sensors, and soft actuators [5-6]. However, one of the challenges in soft robotics is to find suitable materials that can exhibit both mechanical and electrical properties, such as conductivity, elasticity, and durability. Conductivity is essential for soft robots that need to sense their environment, communicate with other devices, or perform electrical functions [7]. Additive manufacturing, or 3D printing, enables the digital fabrication of complex geometries using soft-compliant materials, making it a promising manufacturing method for soft robots. 3D printing electrically conductive composites allow the integration of stretchable sensors and circuits into soft robotic structures. This could enable rapid design iterations and fabrication of fully functional soft robots with integrated electronics.

Various conductive micro and nano-scale fillers have been incorporated into flexible polymer matrices to print stretchable conductive composites [8-10]. Materials like thermoplastic polyurethane (TPU) and silicone rubber have suitable elasticity and deformability for soft robotic applications but do not conduct electricity independently [11-12]. Adding conductive fillers like carbon black nanoparticles provides pathways for electrical conductivity through the insulating polymer matrix without excessively compromising flexibility [13-14]. This has enabled 3D printing of soft sensors, actuators, and circuitry by fused filament fabrication of conductive composite filaments [15].

The consistency and scalability of the 3D printing process allow fabricating conductive components with complex geometries, embedded wiring, and personalized designs [16-17]. Integration of printed stretchable sensors and actuators could enhance the functionality and adaptability of soft robots without rigid components [18]. For example, printed strain gauges can cover a soft robot's body to provide proprioceptive sensing for control [11]. Printed flexible conductive traces can connect sensors to control circuitry and replace soldered wires prone to detachment from soft structures. Printed electrodes can enable dielectric elastomer actuators that deform in response to applied voltages [8].

However, there remain challenges in optimizing the composition and printing process to achieve the high conductivity required for sensors and circuits without compromising mechanical performance [9]. The adhesion, conductivity, stretchability, and consistency of printed composites depend on factors like filler material, size, loading fraction, distribution, and orientation within the flexible matrix. Effective incorporation of fillers also relies on suitable printing parameters and the resulting microstructures. A systematic understanding of these relationships is needed to design optimized conductive composite materials and print reliable integrated electronics.

This study investigates the influence of shape and deformation on the electrical resistance of 3D-printed conductive flexible specimens. Bending and tensile tests are conducted on diverse geometries printed with a conductive thermoplastic material. The objective is to characterize and understand the electromechanical behavior of 3D-printed conductive materials for soft robotic applications. The results provide insights into developing responsive and adaptive soft devices using 3D printing and conductive materials.

2. MATERIAL AND METHOD

The materials used in this study consisted of a conductive flexible filament (EEL by NinjaTek) and a silicone-based mixture (Dragon Skin). The filament was 3D-printed into various shapes and thicknesses, and the mixture was used as a coating layer. The methods involved bending and tensile tests to measure the electrical resistance of the specimens under different loading conditions.

The conductive flexible filament is a thermoplastic elastomer (TPE) with carbon black particles that provide electrical conductivity. The filament has a diameter of 1.75 mm and a shore hardness of 85A. The electrical resistance of the filament was reported to be 0.6 ohm/cm by the manufacturer.
The silicone-based mixture (Dragon Skin) was obtained from Smooth-On. It is a two-component platinum-cure silicone rubber that cures at room temperature. The mixture has a shore hardness of 10A and a pot life of 20 minutes. The mixture is transparent and can be colored with pigments.

The specimens were designed in honeycomb, rectangular, Z- and S-shapes (Figure 1) to evaluate a range of common geometries widely studied for their mechanical properties and deformation behaviors.

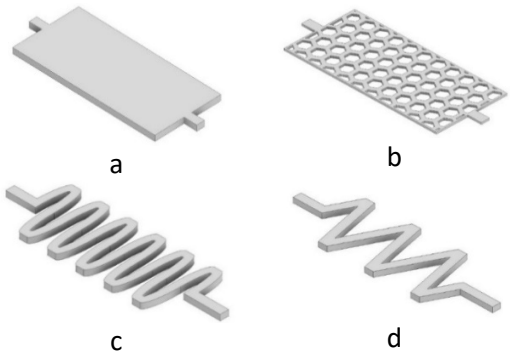

Figure 1. Solid models of the conductive profile designs: a) rectangular, b) honeycomb, c) S-shaped, d) Z-shaped.

These shapes provide established theoretical frameworks and experimental data for benchmarking while also enabling a broad understanding of how geometry affects performance across diverse soft robotics applications. The thicknesses ranged from 0.4 mm to 1.5 mm. The test specimens were 3D-printed using a MakerBot Replicator 2X printer. The printer settings were as follows: nozzle temperature of 230°C, bed temperature of 110°C, extrusion speed of 60 mm/s, layer height of 0.2 mm, and infill density of 100% (Figure 2).

a b

Figure 2. 3D printed test specimens; a) S-shaped, b) rectangular

The silicone-based mixture (Dragon Skin) was used to coat the specimens and form sandwich-like structures. The coating process involved mixing the two components of the mixture in a 1:1 ratio by weight, pouring them into a mold with the desired shape and size, placing the printed specimen in the middle of the mold, filling the rest of the mold with the mixture, and letting it cure for four hours at room temperature. The coated specimens were then taken out of the mold and trimmed to remove excess material. The final specimens had a length of 100 mm, a width of 20 mm, and a total thickness of 2 mm (including the coating layer). Figure 3 shows pictures of the coated specimens.

Conductive filament on soft sensors is the focus of this study, as this area is under-researched. No characterization or data exists on the combination of soft material and conductive flexible filaments on soft sensors. The bending and tensile tests are two basic tests to understand the elasticity versus conductivity profile of soft sensors. The results can be presented as the percentage of elongation, which can approximate the maximum elongation without damage. A similar approach can also provide comparable results for the bending test.

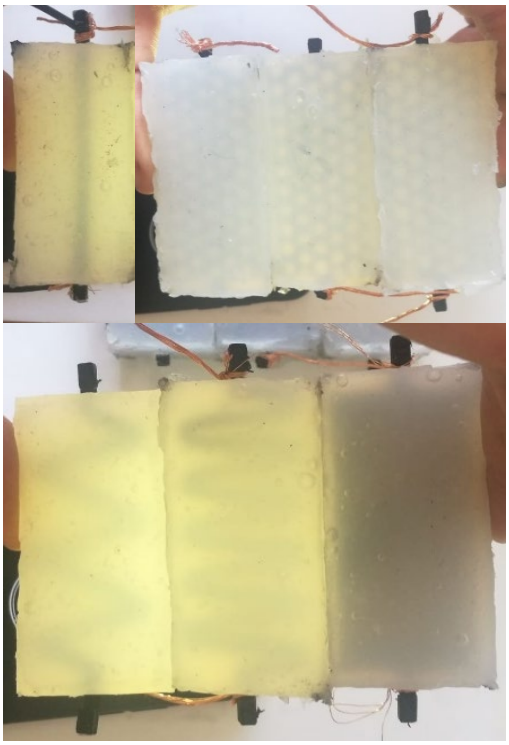

Figure 3. Cured and prepared test specimens.

The tests were standardized by using mountable test setups, calibrated measurement tools, and consistent environmental conditions. A 3D-printed mountable test apparatus was used for the bending test. ABS was chosen as the material for the test setup. Different combinations of length, width, and height were calculated and angles of 30º, 45º, and 60º were obtained. The bending test apparatus was designed in two parts to facilitate mounting and demounting. The upper part had a semicircular shape and was called the forcing part; the lower part had a lunate shape and was called the base part. Figure 4 shows the size comparison of the bending test setup apparatus and Figure 5 shows the bended test specimen.

Figure 4. 3D printed bending test apparatus.

A digital multimeter was used for both bending and tensile test measurements. The tensile test was performed by clamping the test specimen between sliding detachable jaws and securing it with the compressive force of screws. The turning knob was marked to indicate the starting and ending point of one turn. Since one turn corresponded to 1 mm by choosing an M6 bolt, the test specimen was stretched by 1 mm increments.

Figure 5. The test specimen was placed and clamped on the bending test setup.

A tape measure was used to verify the amount of movement and to double-check the accuracy. Insulation was a very critical point for the tensile test, as well as for the bending test. Hot silicone was used as the insulation material, and it was spread on the surface of the jaws that touched the test specimen surface. Figure 6 shows the resistance measurement.

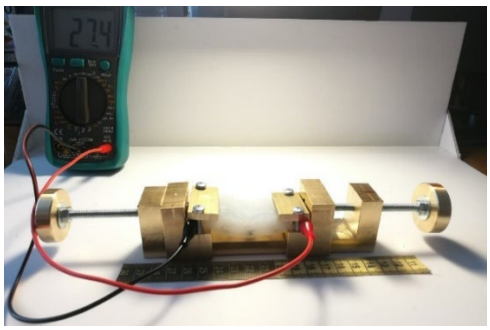

Figure 6. Measurement moment from tensile test on all elements view.

3. RESULTS

The results section demonstrates how different shapes and thicknesses of 3D-printed conductive flexible materials affect their resistance under bending and tensile stresses. The results were presented in graphs and tables with trendlines, comments, and legends. The trendlines were based on the resistance formula that involves area and length as variables. The bending angle and the resistance change were compared for different shape groups. The slope and resistance formulas were used to compare and generalize the results.

3.1. Bending Test Results

The first step of the analysis was to produce honeycomb profiles with different thicknesses: 0.9 mm, 1.2 mm, and 1.5 mm. The specimens were subjected to the same force on different test setups. The data collected from the experiments was plotted on a graph, which is shown in Figure 7.

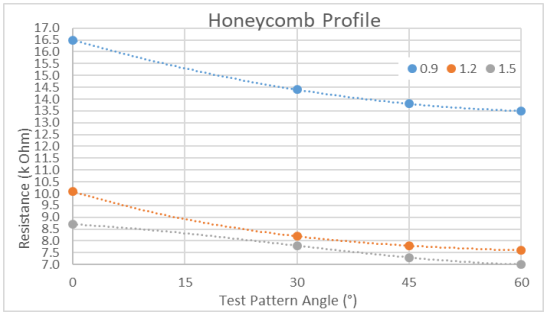

Figure 7. Bending Test Results Graph for Honeycomb Profiles.

The results showed that the resistance of the honeycomb profile specimens decreased as the angle of bending increased. This indicated that there was an inverse proportionality between the bending angle and the resistance for this shape. The thickness of the specimens also affected the resistance change, as thicker specimens showed less sensitivity to bending. Therefore, the resistance and the thickness of the honeycomb profiles had a direct proportionality. Another shape that was tested was the rectangular profile, which had a single thickness of 1.0 mm. The same force was applied to this specimen as to the others, and the results were plotted on a graph in Figure 8.

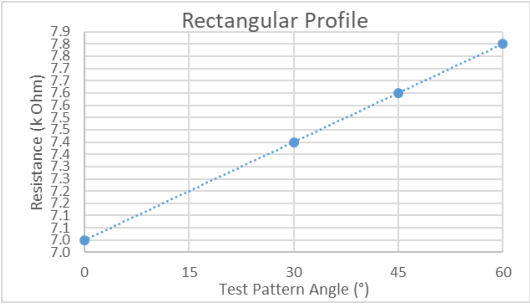

Figure 8. Bending Test Results Graph for Rectangular Profile.

The resistance and the bending angle had a direct proportion for rectangular profiles. The

effect of shapes on the resistance among profiles will be discussed at the end of the section. The "Z" shaped profiles were another group of test specimens with a single thickness of 1.0 mm. The same force was applied to these specimens as to the others. The results are shown in Figure 9.

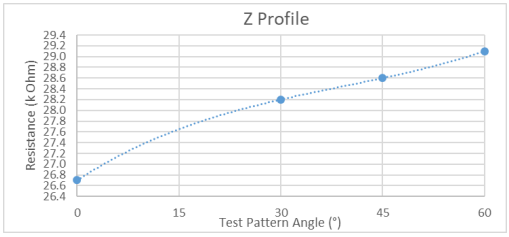

Figure 9. Bending Test Results Graph for "Z" Shaped Profile.

The "Z" shaped profile had a constant thickness, which meant that there was no variation in the thickness. Therefore, the slope and thickness effect could not be examined for this profile. The resistance and the bending angle had a direct proportion for the "Z" shaped profile.

The "S" shaped profile was the last one with a single thickness of 1.0 mm. The same force was applied to this specimen as to the others. The results are displayed in the graph in Figure 10. The profile also had a single thickness, so the slope and thickness effect could not be examined for this profile either. The resistance and the bending angle had a direct proportion for the "S" shaped profile.

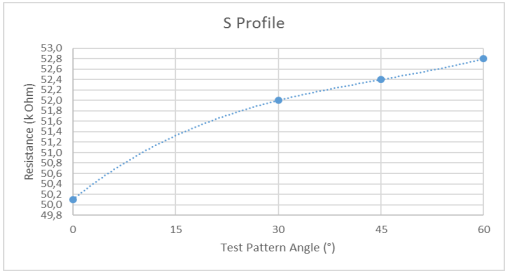

Figure 10. Bending Test Results Graph for "S" Shaped Profile.

3.2. Tensile Test Results

The tensile test results for honeycomb profiles were obtained by applying a constant force to specimens with different thicknesses (0.9 mm, 1.2 mm, and 1.5 mm) and measuring their resistance as they were stretched to the same length. The data were plotted on a graph in Figure 11.

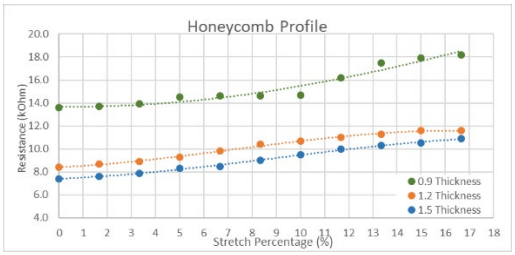

Figure 11. Tensile Test Results Graph for Honeycomb Profiles.

The graph shows that the resistance of the specimens increased as the stretch percentage increased for all thicknesses. This means that there was a direct proportionality between the stretch percentage and the resistance for honeycomb-shaped profiles. The effect of thickness on the resistance change was also evident, as thicker specimens showed higher resistance sensitivity than thinner ones. Therefore, the resistance and the thickness of honeycomb profiles had a direct proportionality as well. Tensile test graphs of rectangular, "Z" shaped, and "S" shaped profiles were given in Figures 12, 13, and 14, respectively.

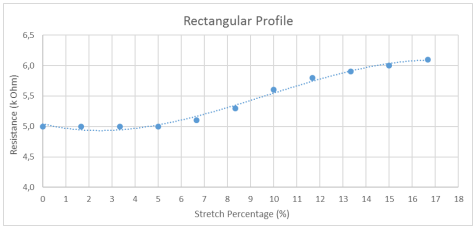

Figure 12. Tensile Test Results Graph for Rectangular Profile.

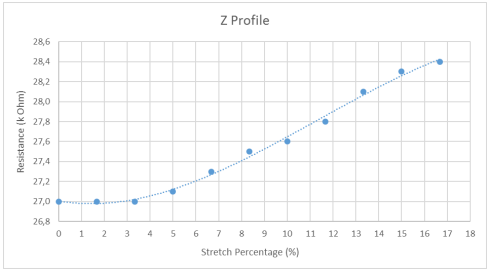

Figure 13. Tensile Test Results Graph for "Z" Shaped Profile.

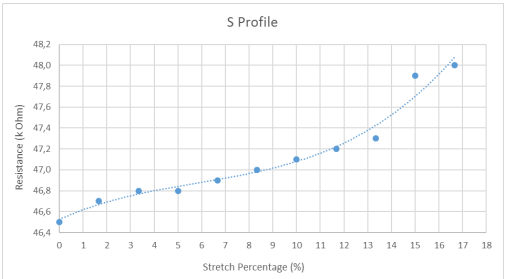

Figure 14. Tensile Test Results Graph for "S" Shaped Profile.

$$\rho = \frac{(R\ x\ A)}{L} \quad (1)$$

The results show how the resistance of 3D-printed conductive flexible materials varies depending on their shape, thickness, bending angle, and stretch percentage. The results are based on bending and tensile tests performed on different geometries of 3D-printed materials using a conductive flexible filament and a silicone-based mixture. The trendlines are derived from Equation (1). The resistivity (ρ) formula shown in Equation 1 is obtained by multiplying resistance (R) with area (A), which is divided by length (L). The area remains constant while stretching due to the relationship between increasing length and decreasing width. Since resistivity should be constant for material, resistance increases with increasing stretch due to an increase in length.

The main findings of the study can be summarized as:

- The resistance is inversely proportional to the thickness for all shapes. This can be explained by the resistivity formula, which states that resistivity equals area times resistance divided by length. Since resistivity is constant for a given material, increasing the area (by increasing the thickness) decreases the resistance. Besides, the relationship between thickness and resistance is found to be the same as in the article of Flowers et al.[13].

- The stretch percentage is directly proportional to the resistance for all shapes except for straight-line profiles. This can be explained by the fact that stretching the material increases its length and decreases its thickness, which both increase the resistance according to the resistivity formula.

- The bending angle is directly proportional to the resistance for "S," "Z," and rectangular shapes and inversely proportional to the resistance for honeycomb and straight-line profiles. This can be explained by the change in the cross-sectional area of the specimens under bending stress. While the ratio of area divided by length (A/L) for "S," "Z," and rectangular shapes decreases with bending, the same ratio increases for honeycomb and straight-line profiles because of their inner structural differences.

- The honeycomb profiles show the most linear relationship between resistance and bending angle or stretch percentage among all shapes. This makes them suitable for 3D-printed soft conductive sensors, as linearity is desirable for sensitivity and accuracy.

These results provide valuable insights into the behavior of 3D-printed conductive flexible materials under different loading conditions. The results can be used to design and develop adaptive and responsive devices for various industries, such as soft robotics, biomedical devices, wearable sensors, and soft actuators. The results also suggest possible directions for future research, such as testing different materials, printing parameters, shapes, and thicknesses, as well as improving the insulation quality and method of the test setups.

4. CONCLUSION

In this study, different shapes with various thickness combinations were examined in two different test setups. The experimental data revealed the effects of thickness, stretch percentage, and bending angle on the resistance of 3D-printed conductive flexible materials. The resistance was found to be inversely proportional to the thickness for all shapes. The stretch percentage was found to be directly proportional to the resistance for all shapes except for straight-line profiles, while the bending angle was found to be directly proportional to the resistance for "S," "Z," and rectangular shapes, and inversely proportional to the resistance for honeycomb and straight-line profile. The honeycomb profiles were observed as the most linear ones in the result graphs, and thus they were selected and recommended as the most suitable shape for 3D-printed soft conductive sensors. The findings of this study contribute to the field of 3D printing and conductive flexible materials and open up new possibilities for designing and developing adaptive and responsive devices for various industries.

REFERENCES

1. Yasa, O et al., "An Overview of Soft Robotics", Annual Review of Control, Robotics, and Autonomous Systems, Vol. 6, Pages 1-29, 2023.

2. Rus, D. and Tolley, M. T., "Design, fabrication, and control of soft robots", Nature, Vol. 521, Issue 7553, Pages 467-475, 2015.

3. Majidi, C., "Soft-Matter engineering for soft robotics", Adv. Mater. Technol., Vol.4 Issue 2, Page 1800477, 2018.

4. Ze, Q., Wu, S. et al. "Soft robotic origami crawler." Science advances Vol. 8, Issue13 pages eabm7834, 2022.

5. Wallin, T. J. J., Pikul, J. and Shepherd, R. F., "3D printing of soft robotic systems", Nat. Rev. Mater., Vol. 3, Issue 6, Pages 84-100, 2018.

6. Yazici , M. V., Kahveci, A. , Kiziltas, F. S., Mulayim, N., and Gezgin, E.," Design and Development of a Surgical Robotic Hand with Hybrid Structure", 2018 Medical Technologies National Congress (TIPTEKNO), Magusa: IEEE, Pages 1-4, 2018.

7. Appiah, C., Arndt, C., Siemsen, K., Heitmann, A., Staubitz, A., and Selhuber-Unkel, C., "Living Materials Herald a New Era in Soft Robotics", Adv. Mater., Vol. 31, Issue 36, Page 1807747, 2019.

8. Stoyanov, H., Kollosche, H. M., Risse, S., Waché, R., and Kofod, G., "Soft conductive elastomer materials for stretchable electronics and voltage controlled artificial muscles", Adv. Mater., Vol. 25, Issue 4, Pages 578-583, 2013.

9. Kwok, S. W., Goh, K. H. H., Tan, Z. D., Tan, S. T. M., Tjiu, W. W., Soh, J. Y., and Goh, K. E. J. "Electrically conductive filament for 3D-printed circuits and sensors", Applied Materials Today, Vol. 9, Pages 167-175, 2017.

10. Kim, S., Kim, S., Majditehran, H., Patel, DK., Majidi, C., and Bergbreiter, S., "Electromechanical Characterization of 3D Printable Conductive Elastomer for Soft Robotics" 3rd IEEE International Conference on Soft Robotics (RoboSoft). IEEE, 2020..

11. Hwang, Y., Paydar, O. H., and Candler, R. N., "Pneumatic microfinger with balloon fins for linear motion using 3D printed molds", Sensors and Actuators A: Physical, Vol. 234, Pages 65-71, 2015.

12. Selvi, Ö., Telli, İ., Totuk, H. O., and Mıstıkoğlu, S., "3D printing soft robots using low-cost consumer 3D printers", 2019.

13. Flowers, P. F., Reyes, C., Ye, S., Kim, M. J., and Wiley, B. J., "3D printing electronic components and circuits with conductive thermoplastic filament", Additive Manufacturing, Vol. 18, Pages 156-163, 2017.

14. Tang, L., Wu, S., Qu, J., Gong, L., and Tang, J., "A review of conductive hydrogel used in flexible strain sensor", Materials, Vol. 13, Issue 18, p. 3947, 2020.

15. Vignali, E., Gasparotti, E., Capellini, K., Fanni, B. M., Landini, L., Positano, V., and Celi, S. "Modeling biomechanical interaction between soft tissue and soft robotic instruments: importance of constitutive anisotropic hyperelastic formulations", The International Journal of Robotics Research, Vol. 40, Issue 1, Pages 224-235, 2021.

16. Selvi, Ö., Totuk O. H., Mistikoğlu S., and Arslan O., "Strengthening effect of flooding in 3d printed porous soft robotics scaffolds", International Journal of 3D Printing Technologies and Digital Industry, Vol. 5, Issue 2, Pages 293-301, 2021.

17. Muth, J. T., Vogt, D. M., Truby, R. L., Mengüç, Y., Kolesky, D. B., Wood, R. J., and Lewis, J. A. "Embedded 3D printing of strain sensors within highly stretchable elastomers", Adv. Mater., Vol. 26, Issue 36, Pages 6307-6312, 2014.

18. Lo, C. Y., Zhao, Y., Kim, C., Alsaid, Y., Khodambashi, R., Peet, M., and He, X. "Highly stretchable self-sensing actuator based on conductive photothermally-responsive hydrogel", Materials Today, Vol. 50, Pages 35-43, 2021.